

Dissimilarity-based Classification of Multidimensional Signals by Conjoint Elastic Matching: Application to Phytoplanktonic Species Recognition

Émilie Caillault, Pierre-Alexandre Hébert, and Guillaume Wacquet

Université Lille Nord de France,
Laboratoire d'Analyse des Systèmes du Littoral, EA 2600, ULCO,
Maison de la Recherche Blaise Pascal,
50 rue Ferdinand Buisson,
B.P. 699,
F-62228 Calais Cedex, France
name@lasl.univ-littoral.fr

Abstract. The paper describes a classification method of multidimensional signals, based upon a dissimilarity measure between signals. Each new signal is compared to some reference signals through a conjoint dynamic time warping algorithm of their time features series, of which proposed cost function gives out a normalized dissimilarity degree. The classification then consists in presenting these degrees to a classifier, like k-NN, MLP or SVM. This recognition scheme is applied to the automatic estimation of the Phytoplanktonic composition of a marine sample from cytometric curves. At present, biologists are used to a manual classification of signals, that consists in a visual comparison of Phytoplanktonic profiles. The proposed method consequently provides an automatic process, as well as a similar comparison of the signal shapes. We show the relevance of the proposed dissimilarity-based classifier in this environmental application, and compare it with classifiers based on the classical DTW cost-function and also with features-based classifiers.

1 Introduction

The survey of marine ecosystem is a major current concern in our society since its impact is essential for many domains: ecology (biodiversity, production, survey), climate, economy (tourism, resources control, transport). In 2000, Directive DCE adopted by the European Parliament [1] defines the Phytoplankton as a biologic factor for marine quality assessment. In this context, we propose an automatic dissimilarity-based classification method designed to assess the marine water quality by Phytoplankton species classification and counting.

The available signals are fluorescence and scatter parameter scans of each particle detected by a flow cytometer in a marine sample. So our problem comes down to the classification of multidimensional signals, whose shape profile is class-specific. Up to date, this classification is made by visual comparison of the obtained profiles and references ones, or by the inverted microscope method [2][3]. The major difficulty of

discrimination task is that Phytoplankton is a live vegetal species. So its internal structure (pigments, size, nucleus position) varies according to its belonging group but also and above all according to its physiological condition (life cycle, cell or colony) and its environment [4][5]. To make a Phytoplankton classifier system robust to these variabilities, it appears relevant to use an elastic measure to compare two signal profiles. So our approach is based on a classical elastic matching from Sakoe and Chiba (Dynamic Time Warping DTW [6]). This method was largely tested, initially for speech recognition (comparison of 1D time-frequency amplitude patterns) or for handwritten pattern recognition (1D spatial matching) [7].

In order to get a more understandable qualitative measure, simple and comprehensible for any biologist, we adapt the matching cost of this algorithm so as to get a $[0, 1]$ -normalized dissimilarity degree that deals with multidimensional time signals.

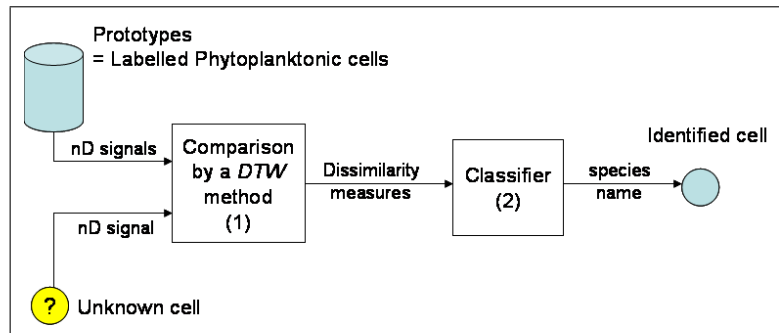


Fig. 1. Scheme of the recognition system for Phytoplanktonic cells

Figure 1 presents the global scheme of the recognition system based on a dissimilarity measure applied to Phytoplankton characterization. It is composed of two classical parts:

1. a feature-like extraction module which computes for the unknown cell a dissimilarity vector in relation to some reference cells;
2. a standard classifier which takes in entry this vector and gives in output the recognized species name.

Next section describes the proposed accommodation of Sakoe and Chiba's algorithm to get a $[0,1]$ -dissimilarity degree between nD signals. Section 3 presents the experimentation protocol and results that show the efficiency of the system with different classifiers. Different variants are tested and compared first with features-based classifiers, then with classical DTW algorithm, in term of recognition rate.

2 Dissimilarity measure for multidimensional signals by conjoint elastic matching

2.1 Comparison of two 1D signals by the classical method *Dynamic Time Warping*

Dynamic Time Warping (DTW) method proposed by Sakoe and Chiba [6] gives a distance measure for two time series, whose lengths are not necessarily equal. This measure represents the quantity of geometrical distortion needed to match both curves, regardless of some time distortions.

More precisely, the method matches the points of both signals, and defines their matching cost as the mean-distance between the paired points. For example, in the ideal case where all paired points are identical, the matching is perfect, and the cost is consequently zero. The softness of the algorithm comes from its ability to pair some points time shifted, with a cost equal to zero.

Let $X = \{(x_i), i = 1, \dots, n_x\}$ and $Y = \{(y_j), j = 1, \dots, n_y\}$ be the two signals to be compared, with i and j their time index, and n_x and n_y their respective length. We first consider monodimensional signals: each value x_i or y_j belongs to \mathfrak{R} .

The algorithm builds a matching $P = \{(i_k, j_k), k = 1, \dots, n_k\}$ between the points of signals X and Y , according to some time conditions. The resulting matching is defined as the one minimizing the following weighted mean distance C between paired points, based upon some distance d and a weight vector W :

$$C(X, Y, P, W) = \frac{\sum_{k=1}^{n_k} d(x_{i_k}, y_{j_k}) \cdot w(k)}{\sum_{k=1}^{n_k} w(k)} = \frac{Dist(X, Y, P, W)}{\sum_{k=1}^{n_k} w(k)}. \quad (1)$$

Selected conditions of the pairing in this DTW variant are the following:

1. End-Points conditions: first (and last) points of both signals are paired: $(1, 1) \in P$ (and $(n_x, n_y) \in P$);
2. Continuity conditions: all points are matched;
3. Monotonicity conditions: pairs are time ordered: $i_{k-1} \leq i_k$ and $j_{k-1} \leq j_k$.

According to these conditions, each possible pairing may be represented as a path in the bidimensional space of the pairs $\{(i, j), i = 1, \dots, n_x, j = 1, \dots, n_y\}$, i.e. the full set of the possible pairs of points of X and Y . The algorithm then backtracks the optimal matching, going from initial pair $(1, 1)$ to final pair (n_x, n_y) (condition 1) that minimizes the cost C .

Sakoe and Chiba showed that cost C can only be optimized by dynamic programming if denominator $\sum_{k=1}^{n_k} w(k)$ does not depend from matching P . This may be obtained by letting the weight sum equal to $n_x + n_y$, n_x or n_y , for example.

Considering that the weights verify this condition, then an optimal path is a path which minimizes the accumulated distance $Dist$.

If the optimal paths leading to pairs $(i-1, j)$, $(i, j-1)$ and $(i-1, j-1)$ are supposed to be known, then the optimal path leading to pair (i, j) may easily be defined as the one of the three previous paths whose cost is minimal, followed by pair (i, j) . Its cost $Dist$ may be computed in the same way. Now, the optimal paths to the pairs $(1, \dots)$ and

$(\dots, 1)$ are known thanks to conditions 2 and 3. Then, a recursive optimization is used to compute the path corresponding to the best matching between signals X and Y , as well as its cost $Dist$. In practice, it consists in sequentially computing the (n_x, n_y) -sized matrix of costs $Dist(i, j)$, which measures the minimal cost of the path leading to pair (i, j) . The final cost is consequently and directly obtained in the last element (n_x, n_y) of the matrix.

Here is given the part of the algorithm DTW (cf. Algorithm 1) allowing a quick computation of cost C of the optimal path. The path itself may then be retrieved following the way the least cost was computed, from last pair (n_x, n_y) to first pair $(1, 1)$. This is generally used to normalize final cost $Dist(n_x, n_y)$, so as to get the mean distortion measure by matched pair.

In order to get the accumulated distance $Dist$ minimization equivalent to the cost C minimization, the weights are defined according to the *symetric* solution proposed by Sako and Chiba. Let (i_k, j_k) be the k -th pair of matching P :

- $w(k) = 2$, if $k = 1$ or if $(i_{(k-1)}, j_{(k-1)}) = (i_k - 1, j_k - 1)$;
- $w(k) = 1$, otherwise.

Then $\sum_{k=1}^{n_k} w(k) = n_x + n_y$ does not depend on P , and optimizing $Dist(n_x, n_y)$ makes C optimized too.

Algorithm 1 DTW algorithm computing the accumulated distance of the best matching

```

Dist(1, 1) = 2.d(x1, y1)
for all i = 2, ..., nx do
    Dist(i, 1) = Dist(i - 1, 1) + d(xi, y1)
end for
for all j = 2, ..., ny do
    Dist(1, j) = Dist(1, j - 1) + d(x1, yj)
end for
for all i = 2, ..., nx do
    for all j = 2, ..., ny do
        Dist(i, j) = min {Dist(i - 1, 1) + d(xi, yj), Dist(i, j - 1) + d(xi, yj), ...
            ..., Dist(i - 1, j - 1) + 2.d(xi, yj)}
    end for
end for
return Dist(nx, ny)

```

2.2 Neighborhood restrictions of DTW algorithm

The previous version of DTW algorithm allows extremely soft matchings without penalty: the first point of a signal may indeed be matched to the last point of the other one. This is an extreme distortion, that may be avoided by narrowing the possible matched points thanks to a limited time window.

The strictest restriction consists in making each point of the longest signal - denoted X - possibly paired to a unique point of the other signal - denoted Y : the time nearest, once the length of the curves are fitted. This is a "linear" DTW:

$$P = \left\{ (i, j_i^*); i \in \{1, \dots, n_x\}, j_i^* = E \left(1 + \frac{(i-1)}{(n_x-1)}(n_y-1) \right) \right\}, \quad (2)$$

where E denotes the round function.

In this particular case, the distortion is global: the one which fits the duration of both signals. No optimization is required to get the distortion cost.

In order to allow local time distortion, a less restrictive version could be preferred, which limits the matchings through a time window. Its size may be defined as a ratio p of the whole duration:

$$\forall (i, j) \in P, (i, j) \in \{(i, j_i); i \in \{1, \dots, n_x\}, j_i \in [j_i^* - p.n_y, j_i^* + p.n_y]\}, \quad (3)$$

where j_i^* denotes the indice defined in the previous linear matching.

2.3 Dissimilarity measure of positive signals

The cost function provided by DTW is a relative measure, which can not be easily interpreted by itself: it is a mean distance, which depends on the intensities of both signals. In order to make the response similar to the one of a human expert, we prefer a bounded measure of dissimilarity, between 0 and 1. We then propose to replace the distance d with a dissimilarity s , built as a ratio of distances:

$$s(x_{i_k}, y_{j_k}) = \frac{d(x_{i_k}, y_{j_k})}{\max\{d(x_{i_k}, 0), d(y_{j_k}, 0)\}}. \quad (4)$$

In order to make this ratio consistent, we suppose the signals to be positive, otherwise the dissimilarity degree could exceed 1.

Using this measure, the cost function C becomes a mean dissimilarity between paired points, and consequently a global dissimilarity measure for signals.

2.4 Conjoint elastic matching of nD signals

We now consider nD signals $\bar{X} = \{(\bar{x}_i), i = 1, \dots, n_x\}$ and $\bar{Y} = \{(\bar{y}_j), j = 1, \dots, n_y\}$, whose all time measures $\bar{x}_i = \{(x_{ic}), c = 1, \dots, n_c\}$ and $\bar{y}_j = \{(y_{jc}), c = 1, \dots, n_c\}$ belong to $(\mathfrak{R}^+)^{n_c}$. To sum up, each nD signal consists of n_c monodimensional positive signals, identically sampled.

In the classical DTW, we simply consider a Manhattan distance measure:

$$d(\bar{x}_i, \bar{y}_j) = \sum_{c=1}^{n_c} d_{L_1}(x_{ic}, y_{jc}), \quad (5)$$

with d_{L_1} the L_1 -distance. The choice consists in accumulating the distortion measures over the n_c curves.

In our dissimilarity version of DTW, we accumulate dissimilarity measures instead of L_1 -distances for the n_c positive curves, and we then normalize the result:

$$s(\bar{x}_i, \bar{y}_j) = \frac{1}{n_c} \sum_{c=1}^{n_c} s(x_{ic}, y_{jc}). \quad (6)$$

2.5 Matching visualizations

In order to visualize the quality of DTW matching for two 1D signals, both signals are usually plotted on the same figure, while paired points are connected with a segment. The weakness of this technique is that it does not help to assess the dissimilarity between the signals.

Then, we propose an other way to visualize both signals X and Y . Each point of pair $(i_k, j_k), k \in \{1, \dots, n_k\}$ of the optimal matching P is represented by a bidimensional point \hat{x}_k (or \hat{y}_k). The set of pairs is totally ordered, then X-axis values of points \hat{x}_k and \hat{y}_k are set to k , following this time order. Y-axis values simply are the 1D measures x_{i_k} and y_{j_k} , then:

$$\hat{x}_k = (k, x_{i_k}) ; \hat{y}_k = (k, y_{j_k}). \quad (7)$$

Plotting points this way makes easier the perception of the distances or dissimilarities accumulated over the pairs of P , because they are directly measured along the Y-axis. Moreover time distortions are visualized. Note that we used dotted lines to differentiate the time distortions from any initial constant part of the curves.

Figure 2 shows the comparison of two artificial 1D curves according to the variants of DTW algorithm previously described; results are presented as follows:

- two columns: left, Sakoe and Chibas’s original algorithm; right, our variant with a bounded dissimilarity degree;
- three couples of rows, for the different ways of limiting the neighborhood: first the ”linear”, then the ” p -restricted”, and finally the ”no-restricted” variant. Results are presented in the classical way, then in the way we propose.

Matchings visualized in Figure 2 show how similar both types of algorithms are, either distance or dissimilarity oriented: the only significative difference appears in the costs, normalized in $[0,1]$. Furthermore this example attests the role of the neighborhood restriction, that allows limitation of the time distortions.

3 Application to the Phytoplanktonic species identification

3.1 Data presentation

ND signals acquisition. In this study, nD signals were gathered in the LOG laboratory¹ from different phytoplanktonic species living in Eastern Channel, with a CytoSense flow cytometer (CytoBuoy²), and labelled by biologists [3], once having them isolated from the natural environment.

Flow cytometry is a technique used to characterize individual particles (cells or bacteria) driven by a liquid flow at high speed in front of a laser light (cf. Figure 3). Different signals either optical or physical are provided: forward scatter (which reflects the particle length), sideward scatter (which is more dependant on the particle internal structure) and several wavelengths of fluorescence (which depend upon the type of its photosynthetic pigments) measures.

¹ Laboratoire d’Océanologie et de Géosciences, UMR 8187: <http://log.univ-littoral.fr>

² Cytobuoy system: <http://www.cytobuoy.com>

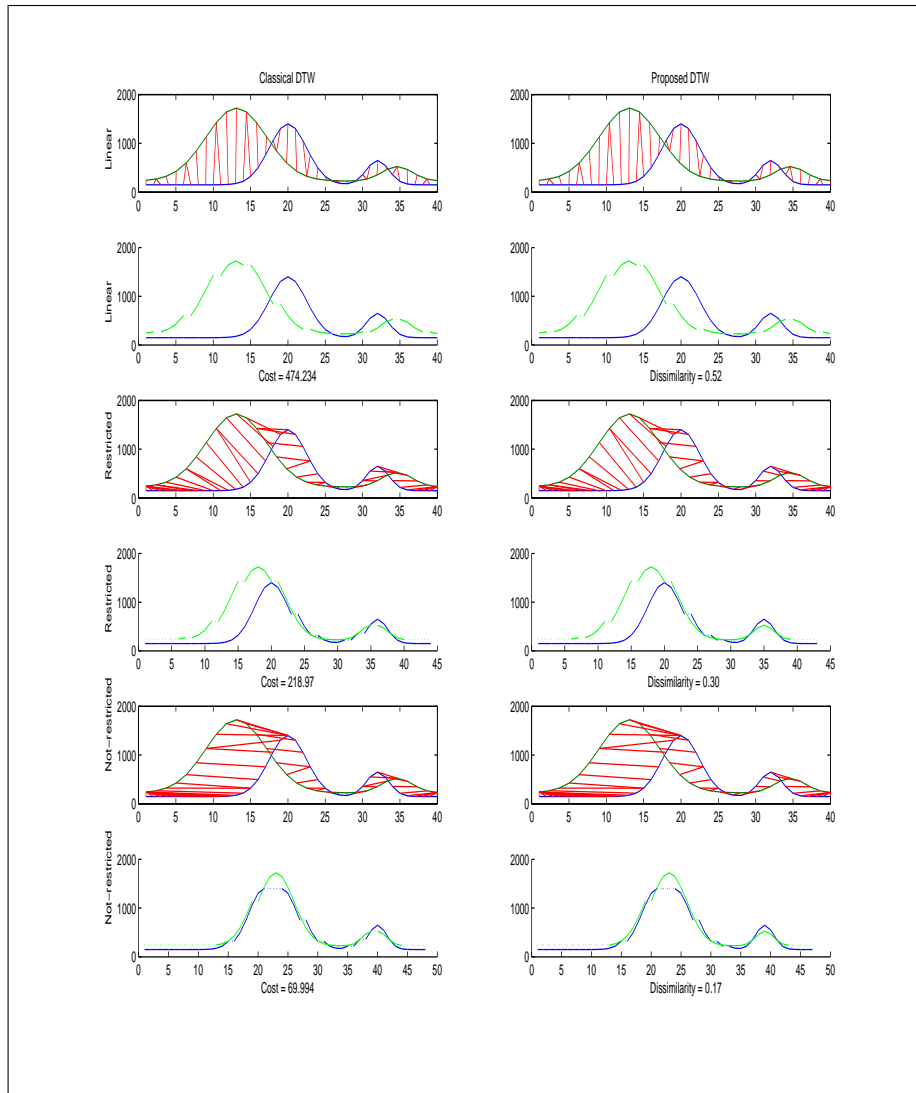


Fig. 2. Different DTW variants applied to two artificial 1D signals

More precisely, in the used signals library, each detected particle is described by 8 monodimensional raw signals issued from the flow cytometer in identical experimental conditions (same sampling rates, same detection threshold, etc.):

- a signal on forward scatter (FWS), corresponding to the cell length;
- two signals on sideward scatter (SWS), corresponding to the internal structure, in high and low sensitivity levels (SWS_HS, SWS_LS);
- two signals on red fluorescence (FLR), $\lambda_{em} > 620nm$, in high and low sensitivity (FLR_HS, FLR_LS), which characterize chlorophyll pigments;

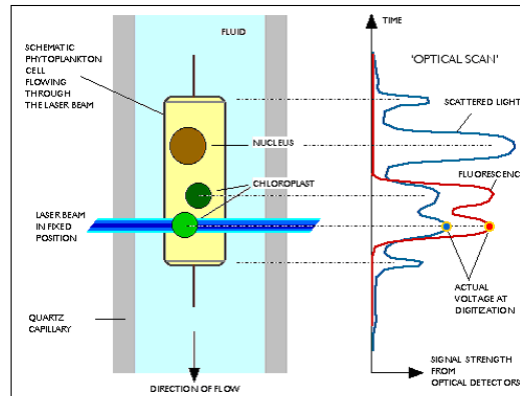


Fig. 3. Signals acquisition with a flow cytometer, image extracted from CytoBuoy's site

- a signal on orange fluorescence (FLO), $565nm < \lambda_{em} < 592nm$, in low sensitivity (FLO_HS);
- two signals on yellow fluorescence (FLY), $545nm < \lambda_{em} < 570nm$, in high and low sensitivity (FLY_HS, FLY_LS).

These signals are composed of voltage measures (mV), and their sampling period was here chosen to correspond to 0.5μ -meter displacement of the water flow. Consequently, the longer the cell is, the higher the number of sampled measures is, and the time axis can be interpreted as a spatial length axis.

Phytoplanktonic species identification is a hard task, that is the reason why all these signals are used to make the particles characterization as complete as possible. Each particle of our experiment is consequently characterized by a 8D signal.

Derived features. Classification process requires an efficient characterization of the particles. This may be obtained either directly from the raw nD signals, or from some features which synthesize information of these signals. 4 attributes per signal are then extracted: length, height, integral, and number of peaks. Each Phytoplankton cell may then be described by 32 derived features.

Description of the studied Phytoplankton cells. The dataset is issued from a unique culture cells sample, whose particles belong to 7 distinct Phytoplanktonic species: *Chaetoceros socialis*, *Emiliania Huxleyi*, *Lauderia annulata*, *Leptocylindrus minimus*, *Phaeocystis globosa*, *Skeletonema costatum* and *Thalassiosira rotula*.

Each species is equally represented by 100 Phytoplanktonic cells, which were labelled by biologists using a microscope [3].

Figures in Table 1 show some signal samples of species *Lauderia annulata* and *Emiliania huxleyi*. For the first species, three individuals are selected: two very close, and an outlier.

Despite a high similarity between the profiles, intra-species variability can be quite important. In particular rising and falling edges of *Lauderia annulata* signals are not

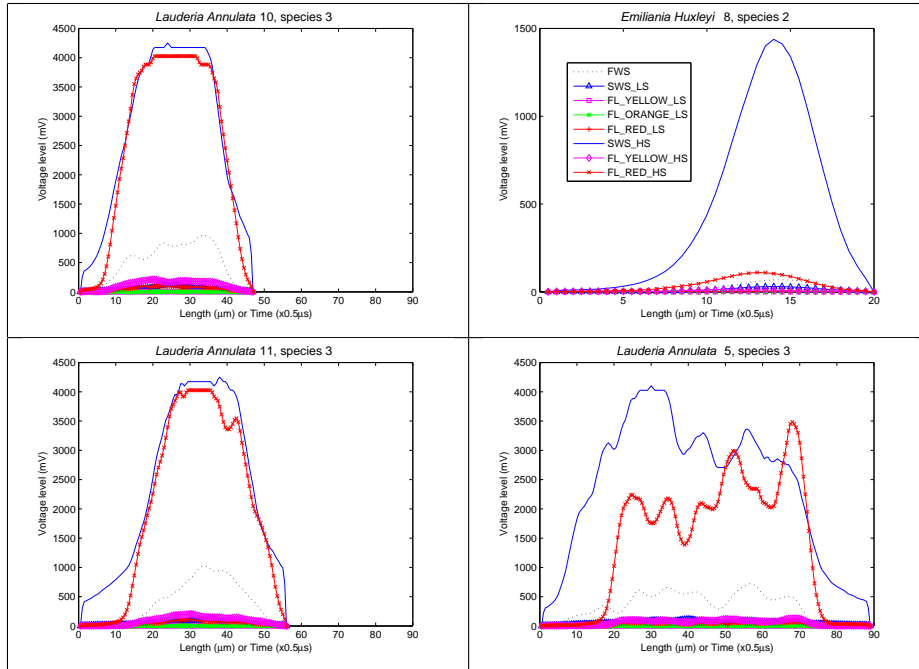


Table 1. nD signals describing two species

exactly synchronous. The curves SWS_HS (the highest ones) of *L. annulata* species show a size variability (*L. annulata* 10: $45\mu\text{m}$, *L. annulata* 11: $55\mu\text{m}$ and *L. annulata* 5: $90\mu\text{m}$), as well as a variability of the nucleus position (at the center of the cell for *L. annulata* 10-11, but clearly left shifted for *L. annulata* 5). In the case of FL_RED_HS signals (the second highest ones), we can also see differences in spatial shifts and in intensity levels between *L. annulata* 5 and the two others: this is due to different positions and different numbers of chloroplasts in cells (cf. Fig. 3).

Last example *E. huxleyi* is an extreme case showing how similar cytometric curves of distinct species can be. However the length of this particle is clearly smaller in this particular case.

3.2 Applied classification methods

Two main classification approaches are experimented:

1. a features-based or "absolute" approach, which consists in applying classical classifiers on the 32 features extracted from the signals;
2. a dissimilarity-based or "relative" approach, which consists in comparing each new Phytoplanktonic cell to a set of labelled cells, directly from its 8 signals, thanks to a DTW variant; the distance or dissimilarity vector is then used as a feature vector, and processed by a classical classifier.

The classifiers are selected among the commonly used:

- k -nearest-neighbor with $k = 1$ (1-NN);
- multi-layer perceptron (MLP), with 1 hidden layer, and the sigmoid transfer function;
- support-vector machine (SVM1), with a first order polynomial kernel;
- support-vector machine (SVM2), with a fourth order polynomial kernel.

DTW-MLP structure used is 175/91/7 neurons (input/hidden/output-layer), features-MLP structure is 32/19/7 neurons. DTW-SVM and features-SVM method used around 300 support vectors in each training fold.

Distance and dissimilarity measures are issued from all the DTW variants previously described:

- first, classical DTW (a mean-distance) versus the proposed DTW variant (dissimilarity-based);
- then, three neighborhood restrictions were compared: "linear", " p -restricted" (with percentage $p = 10\%$ then $p = 20\%$) and the "no-restricted" variants.

In order to better estimate the variability of the recognition scores, 4-fold cross-validation is used: the dataset of 100×7 Phytoplanktonic cells is divided into 4 subsets of 25×7 cells, which are successively used as training fold while the union of the three other subsets is used as a test set.

3.3 Classification results

Features-based classifiers. Table 2 shows the recognition scores of the features-based classification methods. The multi-layer perceptron obtains the best scores (mean score is 95.6%) as well as the least standard deviation (1.1%).

Training fold	Fold 1	Fold 2	Fold 3	Fold 4	Mean	Std
1-NN	93.7	90.2	93.7	92.5	92.5	1.7
MLP	96.9	94.8	96	94.8	95.6	1.1
SVM1	90	87.4	91	92.5	90.2	2.2
SVM2	95	91.2	90	93.9	92.5	2.4

Table 2. Recognition rates (%) of the features-based classifiers

Distance-based and dissimilarity-based classifiers. We now focus on the second approach, based upon the distance and dissimilarity measures. First, classifier 1-NN is used to measure the impact of the neighborhood restriction and the impact of the DTW measure, either classical, or the one proposed. Table 3 shows that the dissimilarity measure reaches higher score than the classical distance measure. This may be explained

by the fact that matched pairs can have extremely high distance, penalizing the final mean-distance cost; but their dissimilarity degree is necessarily bounded by 1: a single badly matched pair can not extremely affect the final mean-dissimilarity cost.

Then, it appears that features-based classifiers scores are surpassed by the dissimilarity-based approaches. This tends to prove that the chosen DTW approach is relevant for this application.

Training folds	Fold 1	Fold 2	Fold 3	Fold 4	Mean	Std
Classical distance-based DTW						
linear	93.3	90.8	94.2	92.1	92.6	1.4
10%-restricted	94.8	92.5	94.8	93.7	94.0	1.0
20%-restricted	96.3	92.9	94.6	93.1	94.2	1.5
no-restricted	96.1	90.2	93.5	91.8	92.9	2.5
Proposed dissimilarity-based DTW						
linear	97.7	94.8	95.0	96.1	95.9	1.3
10%-restricted	97.9	94.6	96.0	96.1	96.1	1.3
20%-restricted	98.2	95.4	96.1	97.1	96.7	1.2
no-restricted	97.3	95.6	96.0	96.9	96.4	0.8

Table 3. Recognition rates (%) of the dissimilarity-based 1-NN classifiers

Then, as expected, the best neighborhood restriction appears to be obtained with a moderate window: $p = 10\%$. Consequently, following comparisons between different classical classifiers are conducted using the 10%-restricted DTW algorithms (cf. Table 4).

Training fold	Fold 1	Fold 2	Fold 3	Fold 4	Mean	Std
1-NN	98.2	95.4	96.1	97.1	96.7	1.3
MLP	98.2	97.3	97.3	96.7	97.3	0.7
SVM1	98.8	95.6	95.6	96.1	96.5	1.6
SVM2	92.3	93.5	93.3	92.9	93	0.6

Table 4. Recognition rates (%) of the 10%-restricted dissimilarity-based classifiers

Table 4 finally shows that the multi-layer perceptron is able to reach the highest mean score (97.3%) , with a very low standard deviation (0.7%).

4 Conclusion

In this paper, we proposed a conjoint dissimilarity [0,1]-measure for signals, based upon their shape. Such a bounded measure makes the interpretation by human users easier, and it can also be more relevant than a simple distance in some applications like the

one presented. This dissimilarity measure was adapted to multidimensional signals, by equally weighting each dimension.

The proposed measure was applied to the automatic classification of Phytoplanktonic cells, which appears to be an innovative method: only few automatic species recognitions have yet been proposed. The experiment was performed on a labelled set of 700 Phytoplankton cells, with 100 cells per species. The quality of the obtained rates (which reach 97.2%) tends to show the relevance of the proposed dissimilarity measure, first in comparison with more classical distortion measures, then in comparison with a feature-based characterization.

These promising results encourage some future works, like the use of other distances (for instance in order to weight the distinct signal dimensions), or like the fusion of this distortion dissimilarity with some other dissimilarity measures (for instance, a duration dissimilarity).

Acknowledgements. The authors thank all the members of the LOG laboratory who took part in the data acquisition of the nD signals data, in particular L. Felipe Artigas, Natacha Guiselin, Elsa Breton, and Xavier Mériaux. The data were collected thanks to project CPER "Phaeocystis Bloom" funded by Région Nord-Pas-de-Calais, Europe (FEDER) and Université du Littoral Côte d'Opale.

They also thank Pr. Denis Hamad and our institute ULCO, for coordinating and earning BQR project "PhytoClas".

References

1. The European Parliament, the European Council: Directive 2000/60/ec of the european parliament and of the council of 23 october 2000 establishing a framework for community action in the field of water policy. Official Journal of the European Communities EN **2000/60/EC** (2000)
2. Lund, J., Kipling, G., Cren, E.L.: The inverted microscope method of estimating algal numbers and the statistical basis of estimation by counting. *Hydrobiologia* **11** (1958) 143–170
3. Guiselin, N., Courcot, L., Artigas, L.F., Jéloux, A.L., Brylinski, J.M.: An optimised protocol to prepare phaeocystis globosa morphotypes for scanning electron microscopy observation. *Journal of Microbiological Methods* **77**(1) (2009) 119–123
4. Cloern, J.E.: Phytoplankton bloom dynamics in coastal ecosystems: a review with some general lessons from sustained investigation of san francisco bay, california. *Reviews of Geophysics* **34** (1996) 127–168
5. Takabayashi, M., Lew, K., Johnson, A., Marchi, A., Dugdale, R., Wilkerson, F.P.: The effect of nutrient availability and temperature on chain length of the diatom, *skeletonema costatum*. *Journal of Plankton Research* **28**(9) (2006) 831–840
6. Sakoe, H., Chiba, S.: Dynamic programming algorithm optimization for spoken word recognition. *IEEE Transactions on Acoustics, Speech, and Signal Processing* **ASSP-26**(1) (1978) 43–49
7. Niels, R., Vuurpijl, L.: Introducing trigraph - trimodal writer identification. In: Proc. European Network of Forensic Handwr. Experts. (2005)